BIOCHEMISTRY
including biophysical chemistry & molecular biology

Article

pubs.acs.org/biochemistry

D_2O Solvent Isotope Effects Suggest Uniform Energy Barriers in Ribulose-1,5-bisphosphate Carboxylase/Oxygenase Catalysis

Guillaume G. B. Tcherkez,*[,†,‡] Camille Bathellier,[†,§] Hilary Stuart-Williams,[§] Spencer Whitney,[§] Elisabeth Gout,[∥] Richard Bligny,[∥] Murray Badger,[§] and Graham D. Farquhar[§]

[†]Institut de Biologie des Plantes, CNRS UMR 8618, Université Paris-Sud 11, 91405 Orsay cedex, France

[‡]Institut Universitaire de France, 103 boulevard Saint-Michel, 75005 Paris, France

[§]Research School of Biology, Australian National University, Canberra ACT 0200, Australia

[∥]Laboratoire de Physiologie Cellulaire Végétale, CEA-Grenoble, 17 rue des Martyrs, 38009 Grenoble cedex, France

Supporting Information

ABSTRACT: D-Ribulose-1,5-bisphosphate carboxylase/oxygenase (Rubisco) is the most abundant enzyme on Earth and is responsible for the fixation of atmospheric CO_2 into biomass. The reaction consists of incorporation of CO_2 and solvent H_2O into D-ribulose 1,5-bisphosphate (RuBP) to yield 3-phospho-D-glycerate. The reaction involves several proton-dependent events: abstraction and protonation during enolization of RuBP and hydrolysis and reprotonation of the six-carbon reaction intermediate (carboxyketone). Although much is known about Rubisco structure and diversity, fundamental aspects of the reaction mechanism are poorly documented. How and when are protons exchanged among substrate, amino acid residues, and solvent water, and could alterations of proton exchange influence catalytic turnover? What is the energy profile of the reaction? To answer these questions, we measured catalytic rates and the $^{12}CO_2/^{13}CO_2$ isotope effect in isotopic waters. We show that with increasing D_2O content, the maximal carboxylation velocity (k_{cat}^c) decreased linearly and was 1.7 times lower in pure D_2O. By contrast, the isotope effect on the apparent Michaelis constant for CO_2 (K_c) was unity, suggesting that H/D exchange might have occurred with the solvent in early steps thereby slowing the overall catalysis. Calculations of kinetic commitments from observed isotope effects further indicate that (1) enolization and processing of the carboxyketone are similarly rate-limiting and (2) the tendency of the carboxyketone to go backward (decarboxylation) is likely exacerbated upon deuteration. Our results thus suggest that Rubisco catalysis is achieved by a rather equal distribution of energy barriers along the reaction.

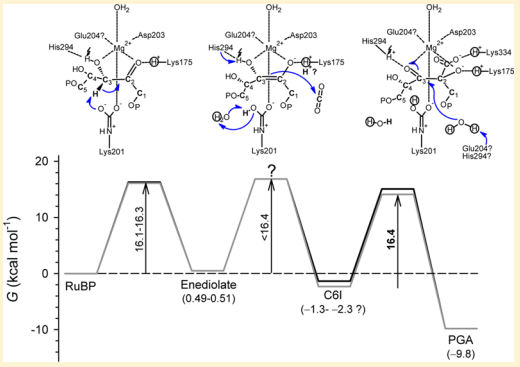

It has now been more than 60 years since D-ribulose-1,5-bisphosphate carboxylase/oxygenase (EC 4.1.1.39, Rubisco) was first purified[1] and 50 years since pioneering experiments dealing with its chemical mechanism were reported.[2] Since then, considerable effort has been devoted to understanding the structure of the active site and the complete reaction mechanism, including the roles of chemical residues (reviewed in ref 3). Rubisco catalyzes the carboxylation (CO_2 addition) or oxygenation (O_2 addition) of D-ribulose 1,5-bisphosphate (RuBP) and the subsequent carbon−carbon cleavage to form two molecules of 3-phospho-D-glycerate (PGA) [with CO_2 (Figure 1, VI)] or one molecule of PGA and one molecule of 2-phosphoglycolate (with O_2). The reaction proceeds through several elemental steps, including enolization, yielding the 2,3-enediolate that is the substrate of CO_2 addition.[4,5] The six-carbon intermediate (carboxyketone) formed is then hydrated,[a,b] cleaved, and reprotonated to yield two molecules of PGA (Figure 1).

In this biologically essential reaction, which abstracts ~120 × 10^9 tons of carbon from the atmosphere each year, key questions remain unanswered, and thus, the perspectives of enzymatic improvement are still limited. Among current uncertainties on Rubisco catalysis are (i) the roles played by several key residues (Lys334, His294, and Glu204), (ii) the origin of the water molecule used for hydration during the reaction, and (iii) mechanisms that make possible unfavorable chemical steps and prevent back-reactions (e.g., decarboxylation of fixed CO_2). Critically, an experiment-based energy profile is lacking, and the dynamics of proton transfers are not well-defined. The enolization step of the reaction, which is believed to be partially rate-limiting,[4,6,7] involves both proton abstraction in H3 (proton attached to C3) and protonation in O2 (negatively charged oxygen atom attached to C2). While proton abstraction is assumed to involve carbamylated lysine 201 (K201), which is the most likely candidate for the base from consideration of crystal structures[8] and also computational methods,[9] the origin and the fate of the proton given to O2 are unclear. On the one hand,

Received: July 16, 2012
Revised: December 21, 2012
Published: January 9, 2013

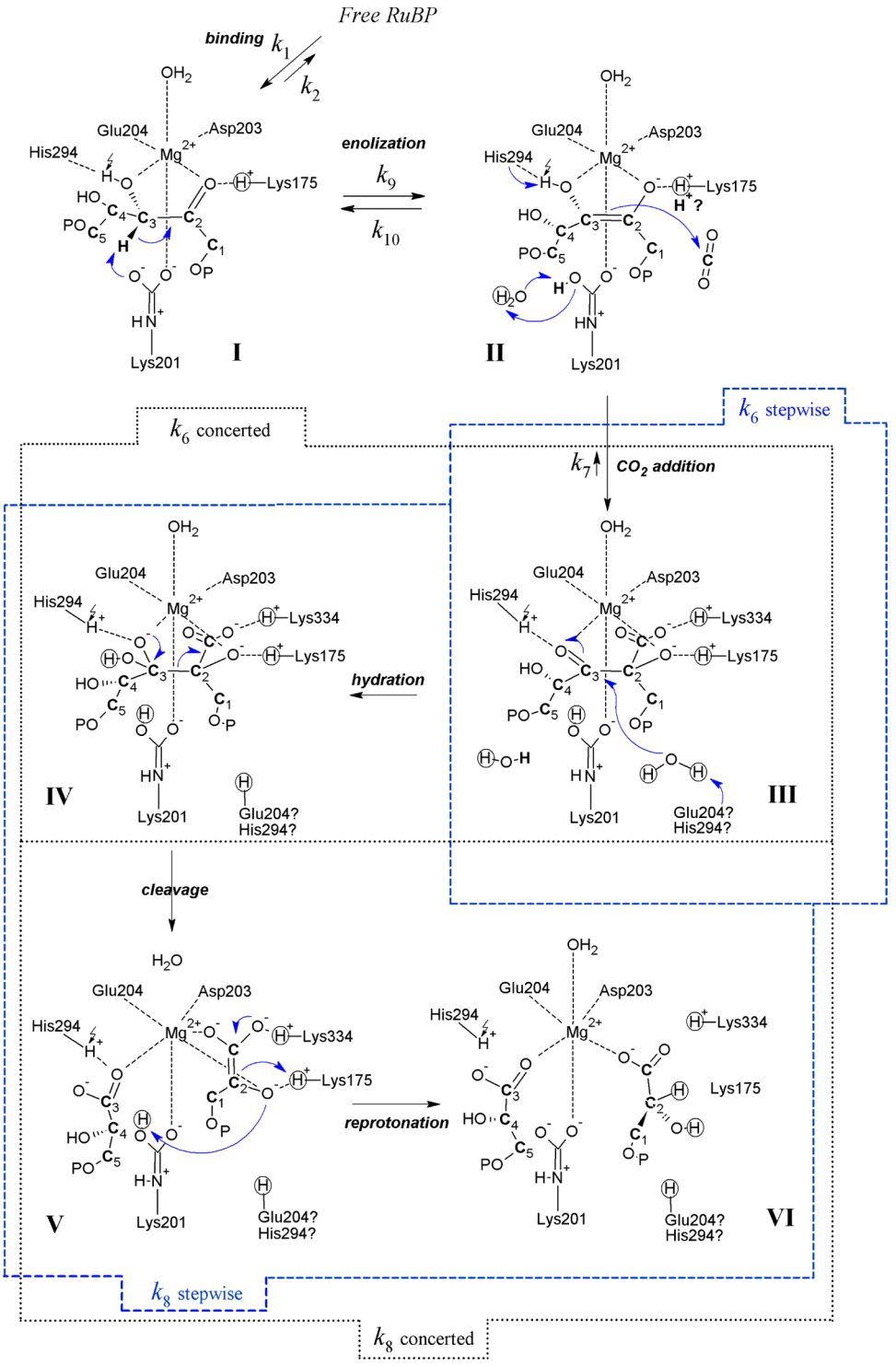

Figure 1. Mechanism of carboxylation of RuBP by Rubisco. This figure is a tentative consensus from refs 10 and 15. The conventional rate constant k_8 is made of three irreversible events (stages III–VI). The fate of protons is emphasized with specific symbols: bold, H3 proton; circles, solvent-derived protons; Z-shaped arrow, O3 proton. Uncertainties are indicated with a question mark. For the sake of clarity, this figure does not show oxygen addition (k_3) and deoxygenation (k_4) or product formation analogous to k_8 (k_5) (for a simplified version of the mechanism, see Figure A1 of the Supporting Information). In this figure, the two possibilities (stepwise vs concerted CO_2 addition and hydration) are shown with frames.

Cleland et al.[10] have suggested that the H3 proton abstracted by carbamylated K201^c may shuttle to O2 and then to K175 and may eventually undergo proton exchange with the solvent. Quite similarly, but during hydration, K175 has been assumed by Mauser et al.[11] to abstract back from O2 the proton donated during enolization. On the other hand, on the basis of the very small enolization activity in the K175G Rubisco mutant (lysine converted to glycine)[12] or computations,[9] it has been suggested that K175 is actually a proton donor.

Downstream in the reaction, protonated K175 may be essential for protonation at C2 of the *aci*-carboxylate of "upper" PGA (i.e., that comes from C1 and C2 of RuBP) during

dx.doi.org/10.1021/bi300933u | *Biochemistry* 2013, 52, 869–877

the last step of the reaction.[10,13,14] Further quantum calculations suggested that K201 and K175 protonate the O2 and C2 atoms, respectively, to form PGA.[15] Still, although it is accompanied by β-elimination (that is, pyruvate production instead of PGA[14]), the K175G mutant has been shown to catalyze forward processing (hydration and cleavage) of the six-carbon intermediate,[12] implying that K175 is not strictly required for terminal protonation.

There is, therefore, no consistent picture of the immediate fate of the proton abstracted during enolization or of the plausible involvement of a proton shuttle between K201 and K175. Furthermore, although a water molecule is commonly thought to be part of the Mg^{2+} coordination sphere,[16] water is believed to be mostly excluded from the chemistry of CO_2 addition and cleavage of the carboxyketone (Figure 1, III). In fact, the binding of RuBP appears to sequester K201 from the bulk, and no water molecule is seen near the carbamate, implying the latter residue experiences a substantially nonaqueous environment.[8,17] The specific role played by protons from solvent water during Rubisco catalysis therefore remains undefined. That said, earlier isotopic investigations with tritium (^3H) or deuterium (D) illuminate somewhat the relationships between RuBP and water protons.

First, the enolization equilibrium does involve protons from water, as shown by substantial isotopic exchange between the C-bound H3 proton and the bulk. With bacterial Rubisco (*Rhodospirillum rubrum*) assayed in tritiated water (^3H_2O) with protio-RuBP, RuBP molecules not consumed by the reaction are eventually fully labeled with ^3H.[6] However, with spinach (*Spinacia oleracea*) Rubisco assayed in D_2O with protio-RuBP, H3 of RuBP molecules was only 31% deuterated.[4]

Second, labeling experiments with tritiated RuBP ([3-^{3}H]RuBP) and spinach Rubisco showed negligible labeling in PGA,[18] and therefore, the H3 proton is commonly believed to be lost before the production of upper PGA (Figure 1, II). That is, reaction intermediates must exchange with the medium at some point during or after enolization. In addition, using D_2O as a solvent instead of H_2O, the reaction catalyzed by the spinach enzyme yields more pyruvate, which comes from β-elimination of the intermediate (competitive with the production of PGA).[19] That is, with a deuterium atom, reprotonation (redeuteration) of C2 (Figure 1, V) is relatively slow, thereby favoring the wasteful cleavage of the carbon−phosphate bond. This shows that the proton used for reprotonation may have exchanged with the solvent, implying the involvement of the proton donor.

The equilibrium associated with enolization (proton abstraction, k_9, and de-enolization, k_{10}) is thus certainly dynamic, favoring proton wash-out to the solvent, possibly involving K175 or other residues.[15] Nevertheless, some difficulties remain in reconciling available experimental data (tangible proton exchange) with structural observations (dry active site around K201). Moreover, isotopic labeling data (with [^{3}H]RuBP) are further complicated by uncertain isotope effects during enolization and its reverse reaction, which presumably favor protio-RuBP over [^{3}H]RuBP.[4,18]

An improved understanding of the chemical path followed by protons during Rubisco catalysis is therefore needed. This would in turn improve our understanding of the energetic balance among the three elemental processes, namely, enolization, CO_2 addition, and processing of the carboxyketone. Here, we conducted assays with spinach Rubisco in both natural (H_2O) and heavy (D_2O) water, with protio-RuBP as a substrate. Kinetic constants as well as the $^{12}C/^{13}C$ isotope effect associated with CO_2 addition were measured in varying H_2O/D_2O isotopic mixtures. Our results strongly suggest that the H/D isotope effect associated with enolization predominates over that associated with hydration, cleavage, and reprotonation (k_8 in Figure 1) in D_2O, supporting the view that isotopic exchange does occur during or just after enolization. Furthermore, we took advantage of isotope effects to calculate commitment factors and show that (i) both enolization and the forward processing of the six-carbon intermediate are similarly rate-limiting for the reaction, (ii) wasteful decarboxylation probably occurs upon substitution of H with D, meaning that the energy barriers of the forward processing and decarboxylation are not very different, and (iii) within the last step of the reaction (forward processing), the rate-limiting event is likely to be protonation of C2. The internal thermodynamics of the enzyme appears to be matched so that free energy barriers are rather similar in the catalytic steady state.

EXPERIMENTAL PROCEDURES

Rubisco Purification, RuBP Preparation, and Rubisco Assays. Rubisco was purified from commercially available spinach (*S. oleracea*) leaves using the method described in refs 20 and 21, omitting the final gel filtration step as in ref 22. RuBP was prepared enzymatically from D-ribose 5-phosphate according to the procedure for unlabeled RuBP described in ref 23. The substrate-saturated turnover rate (k_{cat}^c) and the apparent K_m for CO_2 (K_c) at varying $p(O_2)$ values (to allow calculation of K_o) were measured by $^{14}CO_2$ fixation assays using rapidly extracted soluble leaf protein.[24] Assays were conducted in mixed H_2O/D_2O buffers (see below) equilibrated with N_2 containing 0, 10, or 20% (v/v) O_2. The Rubisco content in the assayed samples was quantified by [^{14}C]CABP (synthesized as described in ref 25) binding, as described in ref 26. $S_{c/o}$ was measured as described previously[27] using [1-^{3}H]RuBP synthesized from [2-^{3}H]-glucose.[37] Tritium in [1-^{3}H]RuBP did not change the specificity via isotope effects (see below). $S_{c/o}$ was calculated as the ratio of ^3H in evolved glycerate and glycolate, taking into account the aqueous solubilities of O_2 and CO_2, and their respective variation with a varying D_2O content.[28,29]

Preparation of H_2O/D_2O Isotopic Waters. Deuterium oxide with a purity of 99.9% (molar percentage) was purchased from the Australian Nuclear Science and Technology Organisation (Sydney, Australia). It was mixed at the appropriate molar ratio to yield 0, 25, 50, 75, or 100% (molar ratio) D_2O. The desired buffer was then prepared (24 mmol L^{-1} triethanolamine-acetic acid, 12 mmol L^{-1} magnesium acetate, and 0.2 mg mL^{-1} bovine erythrocyte carbonic anhydrase) and the solution adjusted to pL 8 (applying the correction to the pH meter reading[30]) using deuterated base (NaOD) or acid (DCl) at the appropriate mixing ratio. Mixed H_2O/D_2O buffers were made shortly before each experiment.

Measurements of $^{12}C/^{13}C$ Signals and Calculation of the $^{12}C/^{13}C$ Isotope Effect. CO_2 uptake in the carboxylation reaction catalyzed by Rubisco was monitored by mass spectrometry using a membrane-inlet system[31,32] (further details of which can be found in Appendix 3 of the Supporting Information). Raw signals were first corrected for the zero offset (baseline) using the baseline value obtained from the five bicarbonate steps injected just before the beginning of the reaction. The classical Craig correction was then applied to the whole data set to convert 45/44 and 46/44 signals into $^{13}C/^{12}C$ ratios. The true $\delta^{13}C$ and $\delta^{18}O$ values for the bicarbonate (measured independently with the IRMS), corrected for the

dx.doi.org/10.1021/bi300933u | *Biochemistry* 2013, 52, 869−877

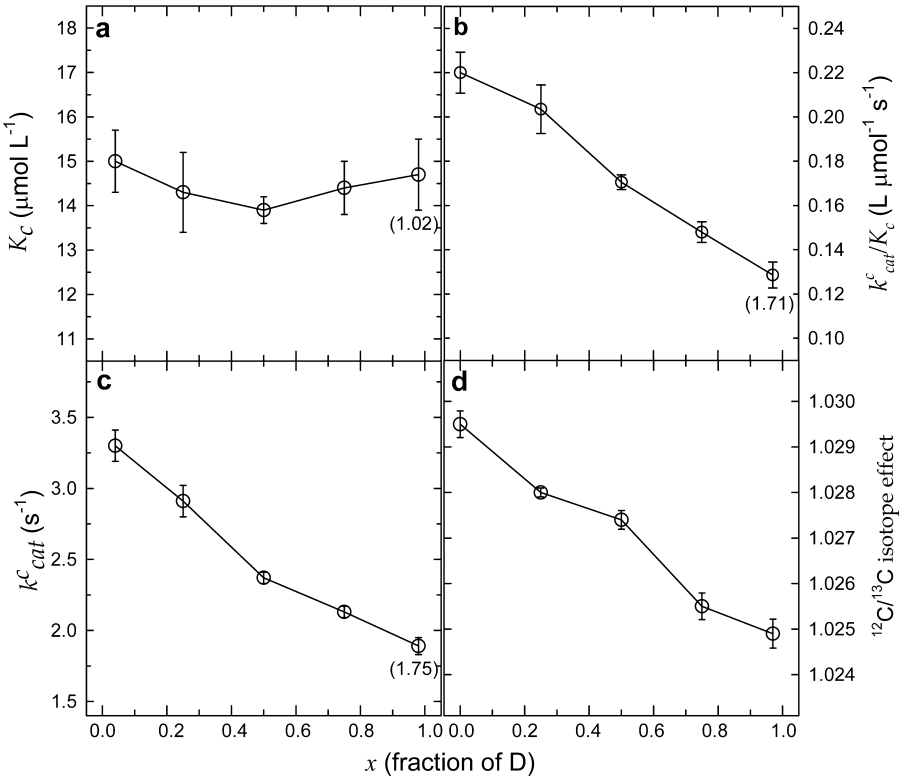

Figure 2. H_2O/D_2O solvent isotope effect and proton inventory on kinetic parameters of carboxylation catalyzed by spinach Rubisco: Michaelis constant (a), catalytic efficiency (b), turnover rate (c), and $^{12}CO_2/^{13}CO_2$ isotope effect associated with net carboxylation with respect to dissolved CO_2 (d). Results are shown vs the deuterium fraction, x (moles of D per mole of H and D). Figures in parentheses are solvent isotope effects (i.e., the value obtained at $x = 0$ divided by that obtained at $x = 1$).

equilibrium isotope effect of acid−base dissociation, were used as a reference to compute the true $^{13}C/^{12}C$ isotope ratio of the reference gas (vs V-PDB). All the data were then corrected against the reference gas to yield absolute $^{13}C/^{12}C$ ratios for all steps of the experiment. Using such corrected ratios, the linearity of the system was checked out with the five bicarbonate additions in the cuvette and a further correction made when necessary. In practice, that correction was minimal and introduced only minor changes. The Rubisco isotope fractionation was then calculated with the Rayleigh equation.[33]

RESULTS

Proton inventory experiments were performed to determine the steps of the catalytic cycle in which solvent-derived protons are involved. By "proton inventory", we mean examination of kinetic parameters in a series of isotopic waters, ranging from normal water (nearly pure protium oxide, H_2O) to pure deuterium oxide (D_2O). In vitro assays allowed us to analyze the kinetic properties of the spinach enzyme (catalytic turnover, k_{cat}; apparent Michaelis constant, K) for both carboxylation and oxygenation. Online mass spectrometric analysis of CO_2 isotopologues was used to measure the $^{12}C/^{13}C$ isotope effect associated with carboxylation.

The "enzymatic efficiency" of carboxylation (k_{cat}^c/K_c) decreased with an increasing deuterium fraction (Figure 2b). The solvent (H_2O/D_2O) isotope effect was 1.71 and was mainly caused by the influence on the turnover rate k_{cat}^c with little effect on Michaelis constant K_c (Figure 2a,c). The kinetic $^{12}C/^{13}C$ isotope effect, $^{13}(k_{cat}^c/K_c)$, of 1.0295 in natural water (effectively H_2O) declined linearly to ∼1.025. This rather small difference between protium- and deuterium-based solvents (4.5‰) shows that the net CO_2 addition rate was only modestly sensitive to the isotopic H/D substitution. This is consistent with CO_2 addition steps per se being water-independent[d] (Figure 1). Nevertheless, the simultaneous decrease in k_{cat}^c and $^{13}(k_{cat}^c/K_c)$ suggests that the steps that terminate the reaction may influence in turn CO_2 addition/decarboxylation steps. Presumably, deuterium substitution makes CO_2 addition either less rate-limiting or more reversible, both possibilities causing $^{13}(k_{cat}^c/K_c)$ to decrease. The specificity of Rubisco toward CO_2 versus O_2 ($S_{c/o}$) was relatively insensitive to D_2O (Figure 3a), with a value of ∼83 in H_2O and ∼79.5 in D_2O. As $S_{c/o} = (k_{cat}^cK_o)/(k_{cat}^oK_c)$ (ref 34), this suggests that oxygenation and carboxylation catalytic cycles were similarly affected by D_2O. In fact, the oxygenation efficiency k_{cat}^o/K_o decreased and was associated with a solvent isotope effect of 1.64 (which is close to the value of 1.71 measured for k_{cat}^c/K_c). The turnover rate of oxygenation (k_{cat}^o) decreased with an increasing deuterium fraction, with a solvent isotope effect of nearly 2 (Figure 3b). The Michaelis constant for O_2 did not show a clear change (Figure 3d), with a statistically insignificant difference between 100% H_2O and D_2O conditions.

All kinetic parameters that were significantly altered by D_2O (k_{cat} and k_{cat}/K) seemed to decrease linearly with deuterium abundance (Figures 2 and 3), and as such, they varied with the first order of deuterium mole fraction, x. That is, the linear character suggests that the solvent isotope effect could have arisen from a single protonic site (see Discussion). This would indicate the involvement of one proton from water per catalytic turnover, with either CO_2 or O_2. It is, however, important to note that this proton inventory carries no direct information about the structural location of the single center that generates the solvent isotope effect. In addition, while the most informative parameters

dx.doi.org/10.1021/bi300933u | *Biochemistry* 2013, 52, 869−877

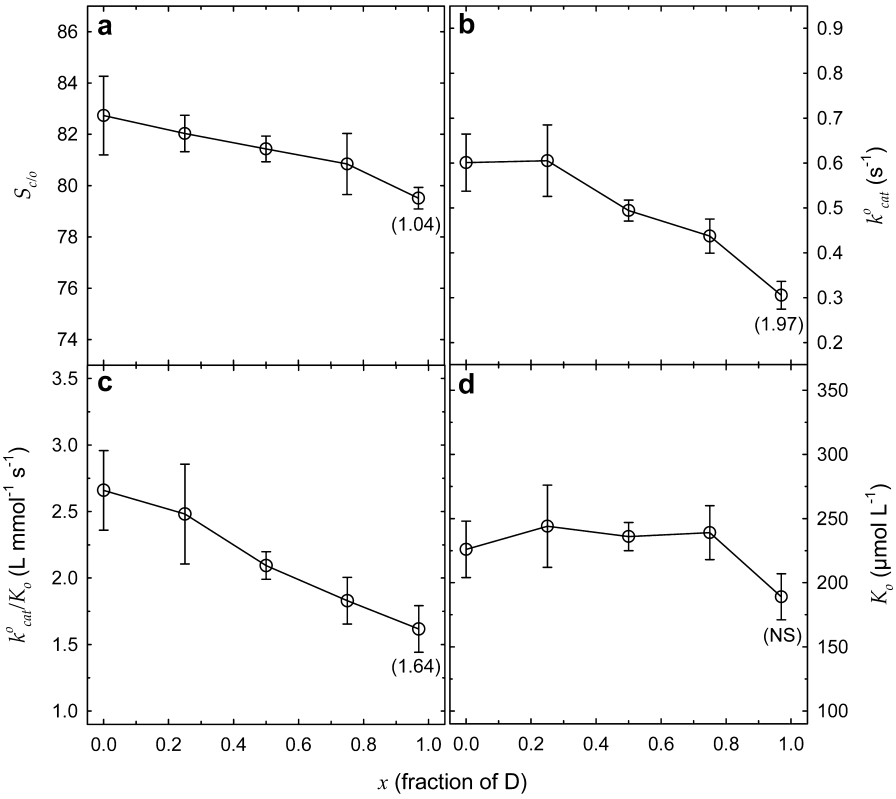

Figure 3. H_2O/D_2O solvent isotope effect on and proton inventory of kinetic parameters of oxygenation catalyzed by spinach Rubisco: CO_2/O_2 specificity (a), turnover rate (b), catalytic efficiency (c), and Michaelis constant (d). Results are shown vs the deuterium fraction, x (moles of D per mole of H and D). Figures in parentheses are solvent isotope effects (i.e., the value obtained at $x = 0$ divided by that obtained at $x = 1$). NS denotes an insignificant solvent isotope effect (not different from 1).

here are k_{cat}^c and k_{cat}^c/K_c, it should be emphasized that they do not correspond to single transition states. That is, they are not equal to individual kinetic constants but to a combination of them. The interpretation addressing this complexity is given below.

DISCUSSION

General Kinetic Relationships. To create a kinetic representation of the catalytic cycle, we use the formal mechanism and rate constants indicated in Figure 1 (further explained in ref 35 and summarized in ref 36) so that the maximal catalytic turnover associated with carboxylation (k_{cat}^c) and the apparent Michaelis constant for CO_2 (K_c) are (for nonlimiting RuBP)

$$k_{cat}^{\ c} = \frac{k_8 k_9}{k_8 + k_9} \tag{1}$$

$$K_c = \frac{k_7 + k_8}{k_6} \times \frac{k_9 + k_{10}}{k_8 + k_9} \tag{2}$$

where k_9 is the rate constant of enolization (forward reaction), k_8 the rate constant of hydration, reprotonation, and cleavage, k_6 the rate constant of CO_2 addition (forward reaction), and k_7 the rate constant of decarboxylation (backward reaction). k_{10} is the rate constant of de-enolization (backward reaction of enolization). In both eqs 1 and 2, it should be noted that we used a common rate constant labeled k_8 for hydration, reprotonation, and cleavage (stepwise CO_2 addition and hydration) or reprotonation and cleavage (concerted CO_2 addition and hydration). We thus assumed (hydration and) reprotonation and cleavage to be a single step or, maybe, concerted steps. If the terminal events were decomposed into separate rate constants, this would not change the conclusions reached below, as both reprotonation and cleavage are irreversible.[37] With H_2O as the solvent, decarboxylation of the C_6 intermediate (k_7) is believed to be very limited (see below and ref 38). The expression of k_{cat}^o and K_o for oxygenation is similar to eqs 1 and 2, in which k_6 is replaced by k_3 (rate constant of O_2-addition) and k_8 by k_5 (rate constant of processing the C_5 intermediate). The reverse reaction of O_2 addition is also believed to be negligible (O_2 fixation is irreversible). Under the assumption that k_7 (decarboxylation) is negligible, eqs 3 and 4 give the H/D isotope effects on k_{cat}^c and K_c, respectively, as follows:

$$^D(k_{cat}^{\ c}) = \frac{\alpha_9 + \alpha_8 \times k_9/k_8}{1 + k_9/k_8} \tag{3}$$

$$^D(K_c) = \frac{^D(k_{cat}^{\ c})}{^D\alpha_6} \times \frac{1 + k_{10}/k_9}{1 + (\alpha_9/\alpha_{10})(k_{10}/k_9)} \tag{4}$$

where $^D\alpha_6$, α_8, α_9, and α_{10} are the intrinsic H/D isotope effects on k_6, k_8, k_9, and k_{10}, respectively. Note that in both eqs 3 and 4, k_6, k_8, k_9, and k_{10} are the rate constants in H_2O and, in D_2O, k_6 becomes $k_6/^D\alpha_6$, etc.[e]

Significance of H/D Isotope Effects. These results demonstrate that there is a solvent isotope effect on k_{cat}^c. If the rate constant associated with enolization were very large ($k_9 \gg k_8$), this would mean the last step (hydration and cleavage, k_8) has an isotope effect of 1.7 (eq 3 and Figure 2). A rather similar value (1.4−1.8) has been found using ^{14}C assays.[18] Here, the proton inventory further seems to suggest that a single site is sensitive to

dx.doi.org/10.1021/bi300933u | *Biochemistry* 2013, 52, 869−877

H/D substitution. Given that, it is worth noting that the linear behavior of k_{cat}^{c} as the deuterium fraction increases (Figure 2) may also come from a linear combination of isotope effects (on both k_8 and k_9), as would be the case in eq 3 where α_8 and α_9 are additive. Because there is no isotope effect on K_c, the rate constants associated with enolization (k_9 and k_{10}) or carboxylation (k_6) are also affected by deuterium [thereby compensating for the isotope effect on k_{cat}^{c} (see eq 4)]. In other words, the use of D_2O may be accompanied by (i) the appearance of deutero-RuBP so that the observed H_2O/D_2O isotope effects result from a combination of rates with isotopically substituted and nonsubstituted RuBP molecules [that is, in the presence of Rubisco, enolization is in dynamic equilibrium and rapidly exchanges protons (and deuterons) between substrate RuBP and the solvent, as already suggested by ref 6] and/or (ii) an isotope effect on carboxylation ($\alpha_6 > 1$), suggesting that water addition and CO_2 addition are concerted.

Previous experiments conducted under symmetrical isotopic conditions (solvent H_2O and [^{2}H-3]RuBP) yielded a $^{D}(k_{cat}^{c}/K_c)$ of 2.0 and a $^{D}(k_{cat}^{c})$ of 2.2 under saturating RuBP conditions (2.2 and 2.6, respectively, under limiting RuBP conditions).[7] Clearly, the values of 2.0 and 2.2 (saturating RuBP) are larger than the value found here (1.7) in D_2O. The lower value obtained here may stem from two opposite causes. First, the isotope effect on enolization (k_9) with deuterated RuBP may impact k_{cat}^{c}, and k_9/k_8 is not very large in eq 3. This would thus mean that during our experiment in D_2O, the isotope effect on k_9 was significant and that on k_8 was <1.7. Second, the isotope effect on k_{cat}^{c} (2.2) came from the deuterium effect on k_8 only, meaning that the deuterium substitution in RuBP directly affected the last step of the reaction. The second hypothesis is less likely, however: isotopic labeling with tritium of H3 has demonstrated that virtually all tritium atoms were lost during the reaction,[18] so the isotopic substitution of H3 cannot influence directly k_8 (see also the introductory section). We therefore conclude that the commitment ratio k_9/k_8 is not very large.

Kinetic Commitments. Advantage can be taken of equations describing isotope effects on rate (described in Appendix 1 of the Supporting Information) by applying them to the results of ref 7 and our own results to determine commitment values that satisfactorily match all the observed isotope effects. Two calculations were conducted (see the Supporting Information for further details): the first is constrained and assumes a stepwise mechanism, with separate CO_2 addition and hydration steps (and thus, hydration is integrated into k_8 and carboxylation itself is not deuterium-sensitive so that α_6 is set to 1); the second assumes that CO_2 addition and hydration are concerted (hydration is integrated into k_6, and thus, we imposed no constraint on α_6). The resulting set of kinetic parameters is shown in Table 1. Enolization appears to be a relatively slow step [$k_9/k_2 < 1$ (Table 1)] associated with a large intrinsic isotope effect of 9−11 and is quite reversible, with a forward-to-backward ratio (k_9/k_{10}) of ∼0.4. The backward reprotonation from the enediolate to RuBP is likely to use partly the H3 proton abstracted during the forward enolization, as evidenced by the fitted isotope effect of only 2 associated with k_{10} with deutero-RuBP as a substrate in ordinary water and close to unity in D_2O. The equilibrium H/D isotope effect associated with proton exchange at H3 of RuBP is expected to be near 1.2. Assuming an intrinsic isotope effect of 9.3 on k_{10} (as for k_9), the estimated percentage of protons derived from RuBP (and not from the solvent) used for de-enolization (k_{10}) would be around $(2.0 - 1)/(9.3/1.2 - 1) \times 100 = 15\%$. In other words, the isotope exchange between the lysine residue and the solvent is not strictly synchronous with enolization, as shown in Figure 1 (step II). Under the assumption that CO_2 addition and hydration are concerted, enolization is hardly affected by D_2O (the calculated exchange factor θ' is zero, and thus, no deuterated RuBP is formed), the isotope effect on carboxylation (k_6) is 1.7, and the kinetic commitment to decarboxylation (k_7/k_8) is zero. In other words, our calculations are such that the lack of a solvent isotope effect on K_c stems from either an effect on enolization (stepwise mechanism) or an isotope effect on carboxylation (concerted mechanism). The last step of the reaction, hydration with reprotonation and cleavage, appears to be sensitive to deuterium ($\alpha_8 > 1$) and partially limiting for catalysis, with a k_8/k_9 ratio of less than unity (Table 1).

Table 1. Kinetic Parameters of the Rubisco-Catalyzed Carboxylation (see the rate constants in Figure 1)[a]

binding	enolization	carboxylation (and hydration)	(hydration and) reprotonation and cleavage
	Kinetic Parameters		
k_9/k_2 0.01[b]/0.22[b]	k_9/k_{10} 0.43[b]/0.43[b]	k_6C/k_{10} >0.4[c]	k_8/k_9 0.83[b]/0.59[b]
θ' 0.38[b]/0.00[b]		k_7/k_8 nd/0.00[b]	
	$^{H}k/^{D}k$ Isotope Effects		
	α_9 9.3[e]/11.0[e]	α_6 (in D_2O) 1[d]/1.7[e]	α_8 (in D_2O) 1.5[d]/2.2[e]
	α_{10} ([D] RuBP) 2.0[e]/2.3[e]	α_7 (in D_2O) nd/0.99[e]	
	α_{10} (in D_2O) 0.8[e]/1.0[e]		

[a]Numbers given here correspond, in that order, to two contrasted assumptions for conducting calculations: CO_2 addition and hydration are stepwise or concerted (corresponding values separated by a slash). nd means not determined. θ' is the isotopic exchange between H3 of RuBP and the solvent (i.e., fraction of exchanged RuBP at equilibrium) in D_2O. [b]Calculated with H/D isotope effects. [c]Roughly estimated with other ratios of catalytic rates (see the text). [d]Imposed (see also the text). [e]Calculated isotope effects.

Several events may simply explain why (hydration and) reprotonation and cleavage is partially limiting and sensitive to D_2O (Figure 4 and Table 1): (i) H_2O dissociation that generates OH^- (nucleophile) for hydration (Figure 1, III) that may be associated with little isotope effect if it is spontaneous[39] or with a significant isotope effect if it is catalyzed by proton abstraction by a basic residue (general base catalysis), (ii) reprotonation of O2, or (iii) reprotonation of C2 (Figure 1, V). Protonation of C2 or O2 with a proton derived from water is likely to be a deuterium-sensitive event. Of course, C2−C3 bond scission itself might involve an isotope effect, but it is far less plausible because no proton transfer is involved (Figure 1, V). Rapid borohydride trapping of the six-carbon intermediate after acid denaturation of the enzyme indicates that the on-enzyme equilibrium favors the hydrated product (gem-diol) by at least 20/1.[37] Because it is unlikely that the latter would accumulate if the subsequent steps were very rapid, hydration itself is not likely to be strongly limiting. Should C2 reprotonation and/or C2−C3 bond cleavage be significantly limiting and thus cause an isotope effect, the causes are believed to be mostly thermodynamic, that is, the low energy level of both the six-carbon intermediate and the gem-diol[36] and the intrinsically high energy level of the transition state associated with C2−C3 bond cleavage.[15]

dx.doi.org/10.1021/bi300933u | Biochemistry 2013, 52, 869−877

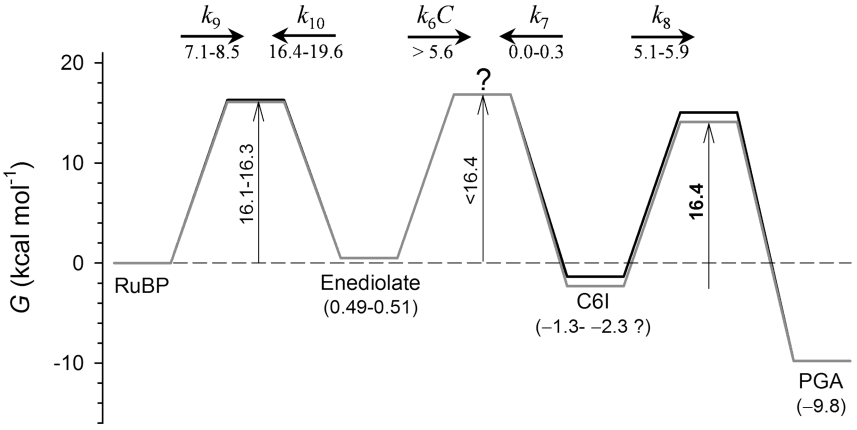

Figure 4. Tentative relative kinetic profile based on commitments calculated here. Note that this is a "kinetic barrier diagram" rather than a classical energy profile;[42] that is, we write second-order rate constants (here, k_6C) as pseudo-first-order constants by including the substrate concentration. Backward reactions (k_{10} and k_7) are simply indicated with arrows pointing to the left. Estimates of rates are calculated from energy barriers with the equation $k = k_BT/h \exp(-\Delta G^{\ddagger}/RT)$ (in s^{-1}) and adjusted to have $k_{cat}^{c} = k_8k_9/(k_8 + k_9) = 3.25\ s^{-1}$ (see Figure 2). The kinetic profiles obtained under the stepwise and concerted mechanism hypotheses are shown with black and gray lines, respectively. The corresponding range of rate constants is shown. Because calculations provide a k_7/k_8 ratio of 0 [concerted mechanism (Table 1)] that would yield an infinite energy barrier, a ratio of 0.01 was used here to provide realistic numbers.

Kinetic Energy Profile. Under the assumption that kinetic constants are given by the equation $k = \kappa k_BT/h \exp(-\Delta G/RT)$, the ratio of two rate constants k_i and k_{ii} gives difference in free energy: $RT \ln(k_i/k_{ii}) = \Delta\Delta G_{ii-i}$. Using the values found here (Table 1), the kinetic profile of the reaction was reconstructed (for a similar example, see ref 40) with the energy barrier of one step fixed at a certain value (Figure 4). The effective free energy barrier of the turnover rate (k_{cat}^{c}) is around 16.8 kcal mol^{-1}, and therefore, the ΔG of the last step (k_8) is estimated to be 16.4 kcal mol^{-1} (see Appendix 2 of the Supporting Information for further details). We recognize that absolute ΔG values may be estimated crudely here, but we believe that this kinetic profile is useful from a qualitative point of view for conducting comparisons. The energy barrier associated with enolization (16.3 kcal mol^{-1}) is smaller than that (17.4 kcal mol^{-1}) obtained by computation and acknowledged by the authors as being conservatively high.[9] The energy difference between the enediolate and RuBP of 0.5 kcal mol^{-1} is reasonably consistent with the energy difference of 0.9 kcal mol^{-1} between ribulose and the associated enediolate in solution.[41] The energy barrier of CO_2 addition (k_6) or of decarboxylation (k_7) of the six-carbon intermediate [2-carboxy-3-ketoarabinitol bisphosphate, or its hydrated form (gem-diol)] back to the enediolate cannot be properly estimated here because the commitment k_6C/k_{10} is not an output of our calculations, but both computational and experimental data (see also Table 1) suggest that k_7 is very small.[15,38] In other words, the energy barrier associated with decarboxylation is not well-known, but the forward processing of the six-carbon intermediate, hydration with reprotonation and cleavage, appears to be energetically favored.

Does Decarboxylation Occur? Although the enzyme appears to have reached optimality by distributing rather similar energy barriers along the reaction (Figure 4) (Knowles theory[42]), the kinetic efficiency of the enzyme yielding PGA seems to be fragile. In addition to reprotonation and cleavage being limiting, energetic alterations might easily disfavor these steps and trigger decarboxylation. The slight decrease in the $^{12}C/^{13}C$ isotope effect ($^{13}\alpha$) and in $S_{c/o}$ may be caused by either the appearance of decarboxylation or a change in the transition state associated with CO_2 addition.[36] However, if D_2O affected the transition state of the carboxylation step and made k_6 more limiting, an increased $^{13}\alpha_6$ would be expected, in contrast to observations (Figure 2). It has been shown that[35,43]

$$S_{c/o} = \frac{k_6}{k_3} \times \frac{1 + k_4/k_5}{1 + k_7/k_8}$$

$$^{13}\alpha = {}^{13}\alpha_6 \times \frac{1 + \frac{k_7}{k_8{}^{13}\alpha_7}}{1 + \frac{k_7}{k_8}}$$

where k_4/k_5 and k_7/k_8 are the commitments to deoxygenation and decarboxylation, respectively, and the intrinsic isotope effects of carboxylation and decarboxylation are $^{13}\alpha_6$ and $^{13}\alpha_7$, respectively. In H_2O, the commitment to the reverse reaction (k_7/k_8) is small (experimentally near 0.05,[38] and here, calculations give 0) and the observed $^{12}C/^{13}C$ isotope effect is 1.029; with a typical carbon isotope effect of 1.040 for decarboxylation ($^{13}\alpha_7$),[44] the intrinsic isotope effect of carboxylation is thus near 1.031. If we assume that α_6 is not affected by D_2O (stepwise mechanism), the decreased $^{12}C/^{13}C$ effect (1.025) suggests that $k_7/k_8 = 0.19$. In other words, the isotopic H/D substitution, which disfavors forward processing of the carboxyketone, may promote decarboxylation. This view would agree with the finding that destabilization of (one of) the transition state(s) associated with hydration, reprotonation, and cleavage (k_8) in the L335V tobacco Rubisco mutant also promoted decarboxylation and decreased the observed $^{12}C/^{13}C$ isotope effect.[45] Furthermore, the equation given above in which $k_7/k_8 = 0.19$ (D_2O) and 0.05 (H_2O) gives a solvent isotope effect on specificity $S_{c/o}$ of 1.13, which is akin to the value observed here [1.04 (Figure 3a)]. Nevertheless, the calculated solvent isotope effect on k_7 ($^{D}\alpha_7$) is here found to be close to unity (Table 1), but it is noteworthy that a large uncertainty remains on calculated k_7/k_8 because of its sensitivity with respect to input data (see the Supporting Information).

Are CO_2 Addition and Hydration Concerted? A specific discussion has already been published elsewhere.[10] Because the production of the keto group (Figure 1, III) appears to be incompatible with partial neutralization of the ionized hydroxyl group by Mg^{2+} coordination, a direct, concerted attack by OH^- at

dx.doi.org/10.1021/bi300933u | Biochemistry 2013, 52, 869−877

C3 may occur at the same transition state as attack on CO_2 by C2. Nevertheless, recent computations suggest that back-and-forth proton exchange with His294 may allow facile charge accommodation on O3 and thus stepwise CO_2 addition and hydration.[15] The present experimental results cannot firmly discriminate between the two possibilities (stepwise vs concerted), and our calculations were conducted under both hypotheses (Table 1). However, the decrease of the $^{12}C/^{13}C$ isotope effect in D_2O is not fully consistent with a more rate-limiting carboxylation step, suggesting that CO_2 addition is mostly water-independent. In addition, the lack of significant change in the Michaelis constants for both CO_2 (Figure 2) and O_2 (Figure 3) is simpler to explain with a common isotope effect (i.e., on the enolization equilibrium because k_9 and k_{10} appear simultaneously in K_c anc K_o) rather than coincidental, similar isotope effects on k_6 (carboxylation) and k_3 (oxygenation). Further experiments are nevertheless needed (with, e.g., the $^{16}O/^{18}O$ isotope effect on oxygenation) to provide new insights into these aspects.

CONCLUSIONS

We provide here the first experiment-based kinetic diagram for the Rubisco carboxylation reaction that includes the enolization step and indicates a rather equal distribution of energy barriers along the reaction. Our results thus suggest that enolization and processing of the six-carbon intermediate are similarly rate-limiting for the reaction. The tendency of the carboxyketone to go backward (decarboxylation) is nearly insignificant in ordinary water but might be exacerbated when the processing of the six-carbon intermediate is slowed by deuteration. These results are in contrast with recent density functional theory calculations[15] that suggested unequal energy barriers and suggested that the processing of the carboxyketone was energetically much disfavored compared to decarboxylation. In addition, our results show a rather facile exchange of protons (involved in hydration and reprotonation) in the active site with the solvent, as revealed by the H/D isotope effect.

We nevertheless recognize that our conclusions may not hold with all Rubisco forms. For the structurally simple homodimeric Rubisco from the prokaryote *R. rubrum*, there is a smaller isotope effect on the maximal carboxylation rate[7] and a larger proton exchange of H3 of RuBP with the solvent,[6] suggesting that both k_8/k_9 and k_2/k_9 are larger than in higher plants. Future studies extending this work to examine other Rubisco forms and the influence of biological origin are therefore warranted. Indeed, our results suggest that rather than Rubisco optimizing a one-dimensional compromise between k_8 and k_6,[46] there is evolutionary pressure on a number of transition states, including that for enolization (k_9). We as scientists may of course group some parameters conveniently as, for example, the turnover (k_{cat}^c), Michaelis constant (K_c), or specificity ($S_{c/o}$). Gaining insight into such adaptive pressures demands an understanding of how photosynthesis is limited in fluctuating natural environments but also a rigorous understanding of chemical constraints.

ASSOCIATED CONTENT

Supporting Information

Principles of calculations for isotope effects and commitments (Appendix I), energy barriers (Appendix II), and methodological details (Appendix III). This material is available free of charge via the Internet at http://pubs.acs.org.

AUTHOR INFORMATION

Corresponding Author

*Institut de Biologie des Plantes, CNRS UMR 8618, Université Paris-Sud 11, 91405 Orsay cedex, France. E-mail: guillaume.tcherkez@u-psud.fr. Telephone: +33 1 69 15 33 79. Fax: +33 1 69 15 34 24.

Funding

This work was conducted with funding from the Australian Research Council and the French Agence Nationale de la Recherche. G.G.B.T. thanks the University Paris-Sud for the postdoctoral fellowship allocated to C.B. and acknowledges the financial support from the Agence Nationale de la Recherche through the project Jeunes Chercheurs, under Contract JC08330055. G.D.F., S.W., and M.B. thank the Australian Research Council for Discovery Grant support.

Notes

The authors declare no competing financial interest.

ABBREVIATIONS

PGA, 3-phospho-D-glycerate; Rubisco, D-ribulose-1,5-bisphosphate carboxylase/oxygenase; RuBP, D-ribulose 1,5-bisphosphate.

ADDITIONAL NOTES

[a] In this paper, we use the notation D for deuterium (^2H) to avoid any confusion with protium (^1H). Isotope effects are thus termed H/D rather than $^1H/^2H$.

[b] Uncertainty remains, however, about whether CO_2 addition and hydration are concerted. This complexity has been addressed in ref 10.

[c] The residue numbering used here refers to spinach Rubisco.

[d] In this section, our reference to CO_2 addition encompasses k_7 as well as k_6.

[e] In eqs 3 and 4, it is assumed that the RuBP concentration is not limiting. If the RuBP concentration were limiting, the isotope effect on carboxylase velocity would be multiplied by an RuBP-dependent term $[1/^D(K)]$. Further description of the equations that account for this is given in the Supporting Information. The Supporting Information also contains full equations, in which k_7 is not neglected. Equation 4 is thus illustrative and not used in calculations.

REFERENCES

(1) Wildman, S. G., and Bonner, J. (1947) The proteins from green leaves. I. Isolation, enzymatic properties, and auxin content of spinach cytoplasmic proteins. *Arch. Biochem. Biophys. 14*, 381−413.

(2) Hurwitz, J., Jakoby, W. B., and Horecker, B. L. (1956) The enzymic formation of PGA from RuDP and CO_2. *Biochim. Biophys. Acta 22*, 194−195.

(3) Andersson, I. (2008) Catalysis and regulation in Rubisco. *J. Exp. Bot. 59*, 1555−1568.

(4) Sue, J. M., and Knowles, J. R. (1982) Ribulose-1,5-bisphosphate carboxylase: Primary deuterium kinetic isotope effect using [3-^2H]-ribulose 1,5-bisphosphate. *Biochemistry 21*, 5410−5414.

(5) Pierce, J., Lorimer, G. H., and Reddy, G. S. (1986) Kinetic mechanism of ribulosebisphosphate carboxylase: Evidence for an ordered, sequential reaction. *Biochemistry 25*, 1636−1644.

(6) Saver, B. G., and Knowles, J. R. (1982) Ribulose-1,5-bisphosphate carboxylase: Enzyme-catalyzed appearance of solvent tritium at carbon 3 of ribulose 1,5-bisphosphate reisolated after partial reaction. *Biochemistry 21*, 5398−5403.

(7) Van Dyk, D. E., and Schloss, J. V. (1986) Deuterium isotope effect in the carboxylase reaction of ribulose-1,5-bisphosphate carboxylase oxygenase. *Biochemistry 25*, 5145−5156.

(8) Taylor, T. C., and Andersson, I. (1997) The structure of the complex between Rubisco and its natural substrate ribulose-1,5-bisphosphate. *J. Mol. Biol. 265*, 432−444.
(9) King, W. A., Gready, J., and Andrews, T. J. (1998) Quantum mechanical analysis of the enolization of ribulose-1,5-bisphosphate: The first hurdle in the fixation of CO_2 by Rubisco. *Biochemistry 37*, 15414−15422.
(10) Cleland, W. W., Andrews, T. J., Gutteridge, S., Hartmann, F. C., and Lorimer, G. H. (1998) Mechanism of Rubisco: the carbamate as general base. *Chem. Rev. 98*, 549−562.
(11) Mauser, H., King, W. A., Gready, J. E., and Andrews, T. J. (2001) CO_2 fixation by Rubisco: Computational dissection of the key steps of carboxylation, hydration, and C−C bond cleavage. *J. Am. Chem. Soc. 123*, 10821−10829.
(12) Lorimer, G. H., and Hartman, F. C. (1988) Evidence supporting lysine 166 of *Rhodospirillum rubrum* ribulosebisphosphate carboxylase as the essential base which initiates catalysis. *J. Biol. Chem. 263*, 6468−6471.
(13) Knight, S., Andersson, I., and Bränden, C. I. (1990) Crystallographic analysis of ribulose 1,5-bisphosphate carboxylase from spinach at 2.4 Å resolution: Subunit interactions and active site. *J. Mol. Biol. 215*, 113−160.
(14) Harpel, M. R., and Hartmann, F. C. (1996) Facilitation of the terminal proton transfer reaction of ribulose-1,5-bisphosphate carboxylase/oxygenase by active site Lys166. *Biochemistry 35*, 13865−13870.
(15) Kannappan, B., and Gready, J. E. (2008) Redefinition of Rubisco carboxylase reaction reveals origin of water for hydration and new roles for active-site residues. *J. Am. Chem. Soc. 130*, 15063−15080.
(16) Taylor, T. C., and Andersson, I. (1996) Structural transitions during activation and ligand binding in hexadecameric Rubisco inferred from the crystal structure of the activated unliganded spinach enzyme. *Nat. Struct. Mol. Biol. 3*, 95−101.
(17) Andersson, I. (1996) Large structures at high resolution: The 1.6 Å crystal structure of spinach ribulose-1,5-bisphosphate carboxylase/oxygenase complexed with 2-carboxyarabinitol bisphosphate. *J. Mol. Biol. 259*, 160−174.
(18) Fiedler, F., Müllhofer, G., Trebst, A., and Rose, I. A. (1967) Mechanism of ribulose-diphosphate carboxydismutase reaction. *Eur. J. Biochem. 1*, 395−399.
(19) Andrews, T. J., and Kane, H. J. (1991) Pyruvate is a byproduct of catalysis by ribulosebisphosphate carboxylase-oxygenase. *J. Biol. Chem. 266*, 9447−9452.
(20) McCurry, S. D., Hall, N. P., Pierce, J., Paech, C., and Tolbert, N. E. (1978) Ribulose-1,5-bisphosphate carboxylase/oxygenase from parsley. *Biochem. Biophys. Res. Commun. 84*, 895−900.
(21) Edmondson, D. L., Kane, H. J., and Andrews, T. J. (1990) Substrate isomerization inhibits ribulosebisphospate carboxylase-oxygenase during catalysis. *FEBS Lett. 260*, 62−66.
(22) Morell, M. K., Wilkin, J. M., Kane, H. J., and Andrews, T. J. (1997) Side reactions catalyzed by ribulose-bisphosphate carboxylase in the presence and absence of small subunits. *J. Biol. Chem. 272*, 5445−5451.
(23) Kane, H. J., Wilkin, J. M., Portis, A. R., and Andrews, T. J. (1998) Potent inhibition of ribulose-bisphosphate carboxylase by an oxidized impurity in ribulose-1,5-bisphosphate. *Plant Physiol. 117*, 1059−1069.
(24) Sharwood, R. E., von Caemmerer, S., Maliga, P., and Whitney, S. M. (2008) The catalytic properties of hybrid Rubisco comprising tobacco small and sunflower large subunits mirror the kinetically equivalent source Rubiscos and can support tobacco growth. *Plant Physiol. 146*, 83−96.
(25) Pierce, J., Tolbert, N. E., and Barker, R. (1980) Interaction of ribulosebisphosphate carboxylase/oxygenase with transition-state analogues. *Biochemistry 19*, 934−942.
(26) Ruuska, S., Andrews, T. J., Badger, M. R., Hudson, G. S., Laisk, A., Price, G. D., and von Caemmerer, S. (1998) The interplay between limiting processes in C-3 photosynthesis studied by rapid-response gas exchange using transgenic tobacco impaired in photosynthesis. *Aust. J. Plant Physiol. 25*, 859−870.
(27) Kane, H. J., Viil, J., Entsch, B., Paul, K., Morell, M. K., and Andrews, T. J. (1994) An improved method for measuring the CO_2/O_2 specificity of ribulosebisphosphate carboxylase-oxygenase. *Aust. J. Plant Physiol. 21*, 449−461.
(28) Wilhelm, E., Battino, R., and Wilcock, R. J. (1977) Low-pressure solubility of gases in liquid water. *Chem. Rev. 77*, 219−262.
(29) Scharlin, P., and Battino, R. (1992) Solubility of 13 non-polar gases in deuterium oxide at 15−45 °C and 101.325 kPa. Thermodynamics of transfer of non-polar gases from H_2O to D_2O. *J. Solution Chem. 21*, 67−91.
(30) Schowen, K. B., and Schowen, R. L. (1982) Solvent isotope effects on enzyme systems. *Methods Enzymol. 87*, 551−606.
(31) McNevin, D. B., Badger, M. R., Kane, H. J., and Farquhar, G. D. (2006) Measurement of (carbon) kinetic isotope effect by Rayleigh fractionation using membrane inlet mass spectrometry for CO_2-consuming reactions. *Funct. Plant Biol. 33*, 1115−1128.
(32) Tobias, H. J., and Brenna, J. T. (1996) Correction of ion source nonlinearities over a wide signal range in continuous-flow isotope ratio mass spectrometry of water-derived hydrogen. *Anal. Chem. 68*, 2281−2286.
(33) Scott, K. M., Lu, X., Cavanaugh, C. M., and Liu, J. S. (2004) Optimal methods for estimating kinetic isotope effects from different forms of the Rayleigh distillation equation. *Geochim. Cosmochim. Acta 68*, 433−442.
(34) Laing, W. A., Ogren, W. L., and Hageman, R. H. (1974) Regulation of soybean net photosynthetic CO_2 fixation by the interaction of CO_2, O_2 and ribulose-1,5-bisphosphate carboxylase. *Plant Physiol. 54*, 678−685.
(35) Farquhar, G. D. (1979) Models describing the kinetics of ribulose biphosphate carboxylase oxygenase. *Arch. Biochem. Biophys. 193*, 456−468.
(36) Tcherkez, G., Farquhar, G. D., and Andrews, T. J. (2006) Despite slow catalysis and confused substrate specificity, all Rubiscos may be nearly perfectly optimized. *Proc. Natl. Acad. Sci. U.S.A. 103* (19), 7246−7251.
(37) Lorimer, G. H., Andrews, T. J., Pierce, J., and Schloss, V. J. (1986) 2′-Carboxy-3-keto-D-arabinitol 1,5-bisphosphate, the six-carbon intermediate of the ribulose bisphosphate carboxylase reaction. *Philos. Trans. R. Soc. London, Ser. B 313*, 397−407.
(38) Pierce, J., Andrews, T. J., and Lorimer, G. H. (1986) Reaction intermediate partitioning by ribulose-bisphosphate carboxylases with differing substrate specificities. *J. Biol. Chem. 261*, 10248−10256.
(39) Bunton, C. A., and Shiner, V. J. (1961) Isotope effects in deuterium oxide solution. Part II. Reaction rates in acid, alkaline and neutral solution, involving only secondary solvent effects. *J. Am. Chem. Soc. 83*, 3207−3214.
(40) Albery, W. J., and Knowles, J. R. (1976) Free energy profile for the reaction catalyzed by triose phosphate isomerase. *Biochemistry 15*, 5627−5631.
(41) Yalayan, V. A., and Ismail, A. A. (1995) Investigation of the enolization and carbonyl group migration in reducing sugars by FTIR spectroscopy. *Carbohydr. Res. 276*, 253−265.
(42) Burbaum, J. J., Raines, R. T., Albery, W. J., and Knowles, J. R. (1989) Evolutionary optimization of the catalytic effectiveness of an enzyme. *Biochemistry 28*, 9293−9305.
(43) Tcherkez, G., and Farquhar, G. D. (2005) Carbon isotope effect predictions on enzymes involved in the primary carbon metabolism of plant leaves. *Funct. Plant Biol. 32*, 277−291.
(44) O'Leary, M. H. (1989) Multiple isotope effects on enzyme-catalyzed reactions. *Annu. Rev. Biochem. 58*, 377−401.
(45) McNevin, D. B., Badger, M. R., Whitney, S., von Caemmerer, S., Tcherkez, G., and Farquhar, G. D. (2007) Differences in carbon isotope discrimination of three variants of ribulose-1,5-bisphosphate carboxylase/oxygenase reflect differences in their catalytic mechanisms. *J. Biol. Chem. 282* (49), 36068−36076.
(46) Savir, Y., Noor, E., Milo, R., and Tlusty, T. (2010) Cross-species analysis traces adaptation of Rubisco toward optimality in a low-dimensional landscape. *Proc. Natl. Acad. Sci. U.S.A. 107*, 3475−3480.